Label-free detection of DNA hybridization based on hydration-induced tension in nucleic acid films

JOHANN MERTENS[1], CELIA ROGERO[2], MONTSERRAT CALLEJA[1], DANIEL RAMOS[1], JOSE ANGEL MARTÍN-GAGO[2,3], CARLOS BRIONES[2] AND JAVIER TAMAYO[1]*

[1]Bionanomechanics Lab (IMM-CNM), CSIC. 28760 Tres Cantos, Madrid, Spain
[2]Centro de Astrobiología (CSIC-INTA). 28850 Torrejón de Ardoz, Madrid, Spain
[3]Instituto de Ciencia de Materiales de Madrid (CSIC). Cantoblanco, 28049 Madrid, Spain
*e-mail: jtamayo@imm.cnm.csic.es

Published online: 20 April 2008; doi:10.1038/nnano.2008.91

The properties of water at the nanoscale are crucial in many areas of biology, but the confinement of water molecules in sub-nanometre channels in biological systems has received relatively little attention. Advances in nanotechnology make it possible to explore the role played by water molecules in living systems, potentially leading to the development of ultrasensitive biosensors. Here we show that the adsorption of water by a self-assembled monolayer of single-stranded DNA on a silicon microcantilever can be detected by measuring how the tension in the monolayer changes as a result of hydration. Our approach relies on the microcantilever bending by an amount that depends on the tension in the monolayer. In particular, we find that the tension changes dramatically when the monolayer interacts with either complementary or single mismatched single-stranded DNA targets. Our results suggest that the tension is mainly governed by hydration forces in the channels between the DNA molecules and could lead to the development of a label-free DNA biosensor that can detect single mutations. The technique provides sensitivity in the femtomolar range that is at least two orders of magnitude better than that obtained previously with label-free nanomechanical biosensors and with label-dependent microarrays.

The change in the properties of water at the nanoscale is crucial in the structure and intermolecular interactions of biological assemblies[1]. Self-assembled monolayers (SAMs) of single-stranded DNA (ssDNA) probes inmobilized on solid supports form the base of a variety of biosensors and nanoscale devices[2–4]. At high packing conditions, ssDNA molecules align vertically, thereby creating intermolecular channels with sub-nanometre diameters. Although the confinement of water in such channels should play a fundamental role in intermolecular interactions, it has received little attention. However, advances in nanotechnology, in particular micro- and nanomechanical sensors[5–16], can potentially be used to analyse the role played by water molecules in macromolecular interactions[17–19], and could lead to a new generation of ultrasensitive biosensors.

The experimental setup developed to study the forces induced by water confinement in DNA monolayers, as well as all the experimental details, are described in the Methods and the Supplementary Information. In brief, we formed a dense SAM of a thiol-modified 16-mer ssDNA on the gold-coated side of a silicon microcantilever[2,3,12]. The DNA sequence was selected from the human *BRCA1* gene, which can contain mutations involved in breast cancer[20]. The microcantilever was placed in a humidity chamber in which the relative humidity was controlled by setting the ratio between dry and humid nitrogen. A modification of the forces between the anchored DNA molecules translates into a nanomechanical motion (bending) of the cantilever, which was measured by a scanning optical technique recently developed[21].

EFFECT OF HYDRATION OF NUCLEIC ACID SAMS ON THEIR TENSION

Figure 1 shows surface stress variation as a function of the relative humidity in a hydration/dehydration loop for a ssDNA sensitized cantilever. We distinguish three stages in the hydration curve. Stage I occurs during the adsorption of the first water molecules, up to a relative humidity of 5–20%, and is characterized by a sharp rise of the surface stress (tensile stress) by $\sim$40–70 mN m^{-1}. Higher hydration of the ssDNA monolayer leads to a significant decrease of the surface stress, extending up to a relative humidity of 50–70%. In this region of the curve, referred to as stage II, the compressive variation of the surface stress is $\sim$150–200 mN m^{-1}. In the region of higher hydration up to the wet state, the surface stress decreases slightly with relative humidity (stage III). During dehydration, the surface stress does not follow the hydration path. It shows little variation up to a critical value of relative humidity of $\sim$20%, after which it rapidly increases, returning to the initial value of the hydration/dehydration loop. As a reference, the hydration/dehydration loop for the gold-coated cantilever before ssDNA monolayer assembly is plotted. The surface stress shows almost a flat response when the relative humidity is varied. This demonstrates that the significant hydration dependence of the surface stress for the functionalized cantilever arises from the

© 2008 Nature Publishing Group

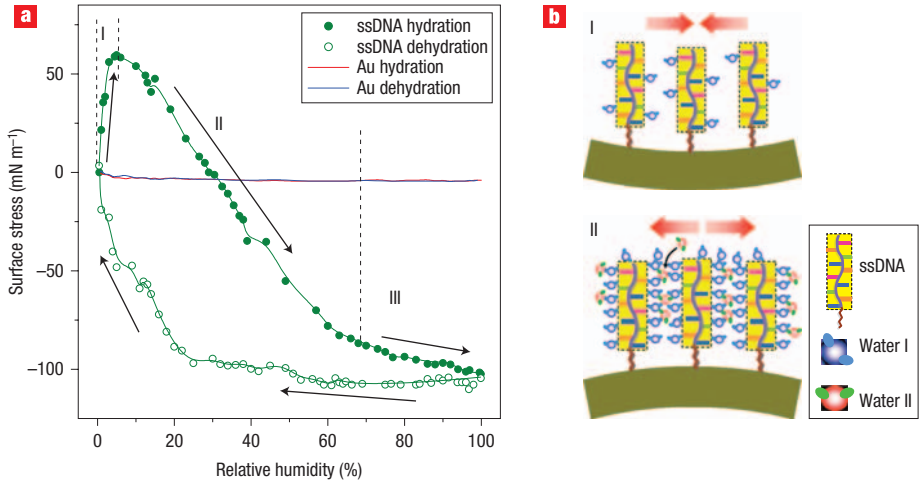

Figure 1 Hydration dependence of the surface stress of densely packed self-assembled ssDNA monolayers. a, Surface stress variation during a hydration and dehydration cycle for a gold-coated silicon cantilever sensitized with a thiol-modified 16-mer ssDNA probe (symbols). The cantilever was incubated with a 1 μM solution of the ssDNA probe diluted in PBS at 24 ºC for 24 h. The cantilever was then rinsed in PBS buffer and Milli-Q water at 24 ºC to discard unspecific interactions, and then dried under a stream of dry nitrogen gas. For comparison, the hydration/dehydration loop for the gold-coated cantilever before functionalization is also shown (red and blue lines). The surface stress variations are measured with respect to the surface stress at a relative humidity of 0. The relative humidity was changed at a rate of about 1% per minute. The ssDNA-sensitized cantilever shows a significant and characteristic surface stress dependence on relative humidity, which is also accompanied by hysteresis in the hydration/dehydration loop (the relevant stages in the surface stress curve during hydration are labelled I, II and III). This dependence is not observed with the gold-coated cantilever. **b**, Schematics of the ssDNA monolayer in stage I and stage II. The ssDNA molecules are anchored to the gold in a standing-up position via the thiol group. The channels between the ssDNA molecules host the adsorption of a few water shells around the DNA molecules. In stage I, the adsorption of the first water molecules (water I) leads to a rapid increase in the surface stress (tensile stress). This arises from the increase in attractive forces provided by the water molecules bound to the ssDNA chains that build the hydration shell. In stage II, the population of water molecules in the intermolecular channels (water II) leads to a repulsive hydration pressure that translates into a compressive change of the surface stress. In stage III, the surface stress slightly decreases with relative humidity. This stage is related to the adsorption of water on top of the DNA films.

interaction between the water and the anchored DNA molecules. Notice that the surface stress at the dry state is set as the zero reference.

The behaviour described above was found exclusively for ssDNA immobilization times of 24–48 h. For shorter immobilization times, the surface stress did not exhibit a noticeable dependence on relative humidity (see Supplementary Information). This suggests that the observed phenomenon requires the formation of a SAM that is standing up, that is, in which the ssDNA molecules are anchored to the surface only by means of their terminal thiol groups[2,3]. Analysis by X-ray photoelectron spectroscopy (XPS) indicates a ssDNA grafting density of about 4×10^{13} molecules per cm^2, with most of the molecules standing up (see Supplementary Information). Assuming that the ssDNA molecules behave as cylinders with a diameter of 1.3 nm and adopt a hexagonal packing configuration, the DNA membrane hosts intermolecular channels with a diameter of about 0.8 nm (see schematics in Fig. 1). The dense packing makes the ssDNA monolayer behave as a molecular membrane, in which the molecules cooperatively adopt a conformation in response to interactions brought about by the insertion of new molecules into the membrane.

The initial hydration (stage I) is linked to the formation of DNA hydration shells, in which the water molecules bind to the ssDNA strands through hydrogen bonds[22,23]. The water in the hydration shells shows differences in its properties compared with the water in bulk solution, such as partial ordering and lower mobility. During this stage, attractive forces (tensile stress) due to dipole–dipole interactions[17–19] may be detected. As the relative humidity increases above 5–20% (stage II), water molecules adsorb between the hydration shells ('water II' in the schematic of Fig. 1), initiating the formation of an intricate hydrogen-bond network. The ssDNA anchorage to the gold by means of the thiol groups restricts the accommodation of the hydrogen-bond network, leading to an increasingly repulsive steric hindrance (compressive stress)[17–19]. Finally, in the third regime of water adsorption (stage III), the small slope of the surface stress curves found at relative humidities >60% strongly suggests the adsorption of water on top of the DNA films, once the intermolecular channels have been filled. A key signature of the response of the ssDNA monolayer is the hysteresis in the hydration/dehydration loop, which indicates that the process is accompanied by energy dissipation, suggesting the existence of capillary-like forces between the ssDNA molecules[24]. In fact, this signature has been found in nanoporous materials, indicating that our membrane model with intermolecular channels is a good approach for understanding the phenomenon[25]. During dehydration, it is only at very low humidity (<20%) that the water molecules are not available in sufficient amounts to maintain the capillary molecular bridges, and the microcantilever tension returns to its initial value.

The next step was to hybridize the ssDNA-sensitized cantilever with 1 μM of complementary ssDNA sequence over 1 h (see Methods). Once the cantilever was hybridized, rinsed and dried, the hydration-induced tension showed a quantitatively and qualitatively different behaviour with respect to that of ssDNA (Fig. 2). First, the surface stress decreased with relative humidity by ~100–150 mN m^{-1} from the dehydrated to the fully hydrated state; that is, the initial increase of the surface stress observed for the ssDNA case vanishes. Second, the hysteresis in the hydration/dehydration loop is largely reduced upon hybridization.

© 2008 Nature Publishing Group

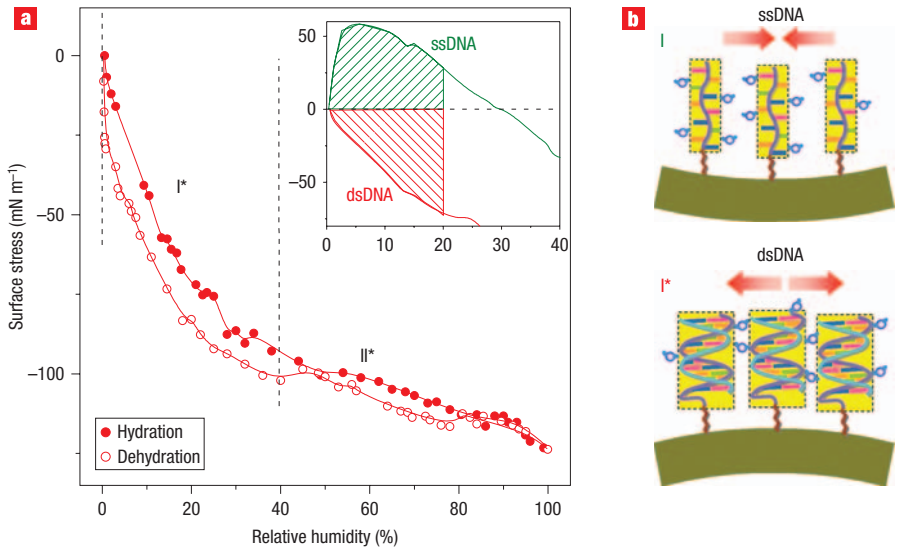

Figure 2 Effect of hybridization on the surface stress versus relative humidity relationship. a, Surface stress is shown during a hydration/dehydration loop for the ssDNA-sensitized cantilever shown in Fig. 1, after exposure to 1 μM of the complementary ssDNA target for 1 h (symbols). The surface stress at a relative humidity of ~0 is chosen as the zero reference. Based on the slope of the surface stress upon hydration, two stages are distinguished. In stage I*, the surface stress significantly decreases between relative humidity levels of 0 and ~40% as a consequence of the shrinking of the intermolecular channels produced by the DNA duplexes formed. The water adsorption in the narrow channels leads to repulsive steric forces. For higher humidity, stage II*, the slight decrease of the surface stress with relative humidity is related to the adsorption of water on top of the nucleic acid monolayer. **b**, Schematics of the DNA monolayer before (ssDNA) and after (dsDNA) hybridization during the initial hydration. The attractive force induced by the initial hydration of the surface-grafted ssDNA molecules turns into a repulsive force after hybridization. This different behaviour is the identifier of DNA–DNA hybridization and it is used to monitor the performance of the biosensor. The inset to **a** shows surface stress versus relative humidity during initial hydration for the ssDNA film and after subsequent hybridization. The hybridization is quantified by the area enclosed by the curves between relative humidities of 0 and 20% (dashed area).

Neither longer hybridization times nor higher concentrations of the complementary target produce a significant change in the described cantilever response. When the sensitized cantilever was exposed to non-complementary DNA, the surface stress response to hydration showed no significant changes with respect to the non-hybridized sensitized cantilever (see Supplementary Information). This implies that specific Watson–Crick base pairing is the key intermolecular interaction that produces the differential phenomena described above.

In Fig. 2, we distinguish stage I*, where relative humidity lies in the range ~0–40% and in which surface stress significantly decreases with relative humidity, and stage II* for higher humidity, where there is a weak dependence on relative humidity. The adsorption of the first water molecules in stage I* produces a repulsive inter-DNA force. This force is related to the formation of DNA duplexes in the biomembrane, which leads to a reduction of the intermolecular channels, and so to a steric hindrance to water intercalation (see schematic in Fig. 2). Notice that this phase is similar to stage II in the unhybridized ssDNA film, which is governed by similar steric interactions (Fig. 1). Stage II* is related to the adsorption of water on top of the nucleic acid monolayer (as in stage III in the ssDNA film). The large reduction in the surface stress hysteresis is related to the repulsive nature of the inter-DNA interactions upon hydration.

To gain further insight into the hydration-induced forces in DNA SAMs, we performed experiments with peptide nucleic acids (ssPNA) derivatized with a cysteine linker to form SAMs on gold-coated cantilevers. PNA is an uncharged synthetic mimic of DNA in which the negatively charged phosphate–sugar backbone is substituted by a peptidomimetic linear polymer, in which the nucleobases are linked in a conformation prone to specifically interact with complementary natural nucleic acids (DNA or RNA). In addition, ssPNA forms densely packed SAMs on gold in ultrapure water without the need of ions, but ssDNA SAMs need to be formed in buffer solution. Therefore, these experiments can shed light on the role of the electrostatic interactions[26,27]. Figure 3 shows the hydration/dehydration loops of surface stress for ssPNA (Fig. 3a) and after subsequent hybridization with the complementary DNA (Fig. 3b). The surface stress response to hydration before and after hybridization retains all the qualitative basic features found for the ssDNA SAMs. This indicates that electrostatic interactions do not play an essential role in the water-mediated intermolecular interactions between nucleic acid molecules at high packing conditions. These observations are consistent with the reported interactions between DNA molecules in solution[17–19]. For intermolecular distances <3 nm, DNA molecules experience a large repulsive force as a consequence of the perturbation of the hydrogen-bond network surrounding the DNA molecules (hydration shells). The force, referred to as hydration force, exponentially increases with a 0.25–0.35 nm characteristic distance and, consistent with our results, exhibits negligible dependence on the ionic strength. This indicates that for high humidity, the interaction between neighbouring DNA molecules on the metal surface could be governed by similar processes to those that occur in solution.

A NUCLEIC ACID BIOSENSOR BASED ON HYDRATION FORCES

Figure 4a shows the temporal evolution of surface stress versus relative humidity during hydration for a ssDNA monolayer exposed to 1 pM of complementary DNA (the dehydration curves were not depicted for the sake of simplicity). Equilibrium

© 2008 Nature Publishing Group

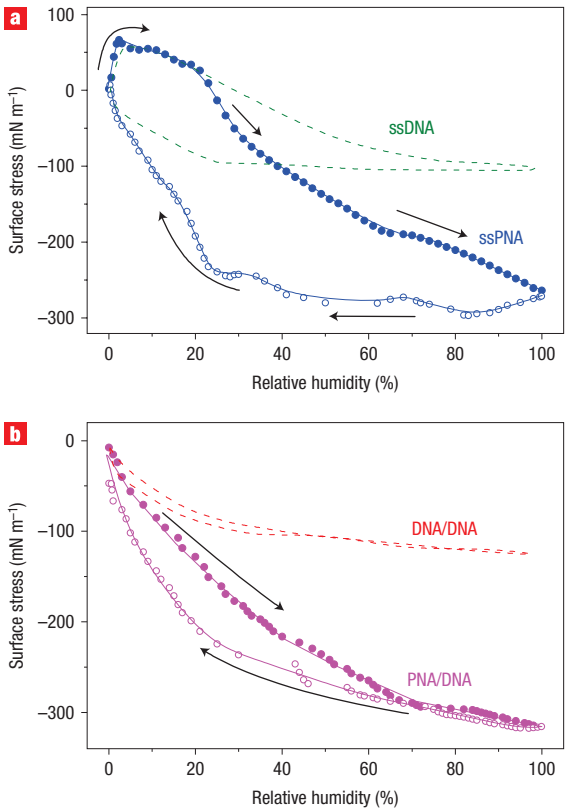

Figure 3 Role of the electrostatic interactions: immobilization of ssPNA probes. a, Surface stress variation during a hydration and dehydration loop of a cantilever sensitized with a Cys-terminated 11-mer ssPNA probe (blue symbols and lines). The curve for the ssDNA film shown in Fig. 1 is also plotted for comparison (green dashed lines). The immobilization was performed with 1 μM of the ssPNA probe diluted in Milli-Q water at 24 °C for 24 h. The cantilever was then rinsed with Milli-Q water to discard unspecific interactions, and then dried under a stream of dry nitrogen gas. **b**, Surface stress variation during hydration and dehydration after exposure of the ssPNA-sensitized cantilever to 1 μM of the complementary ssDNA target (magenta symbols and lines). The curve for the DNA/DNA hybridization shown in Fig. 2 is also plotted for comparison (red dashed line). Whereas DNA is a strongly charged molecule with an effective density of one fundamental negative charge per 0.17 nm of its length, PNA is an uncharged DNA mimic with the phosphate–sugar backbone replaced by a peptidomimetic polymeric structure. In addition, ssPNA forms highly packed SAMs on gold in ultrapure water without the need of ions, but ssDNA SAMs have to be formed in buffer solution. Although the curves for the ssDNA and ssPNA exhibit significant quantitative differences, the shape and the change upon hybridization are qualitatively similar. This indicates that the electrostatic forces are not an essential element in the observed phenomena.

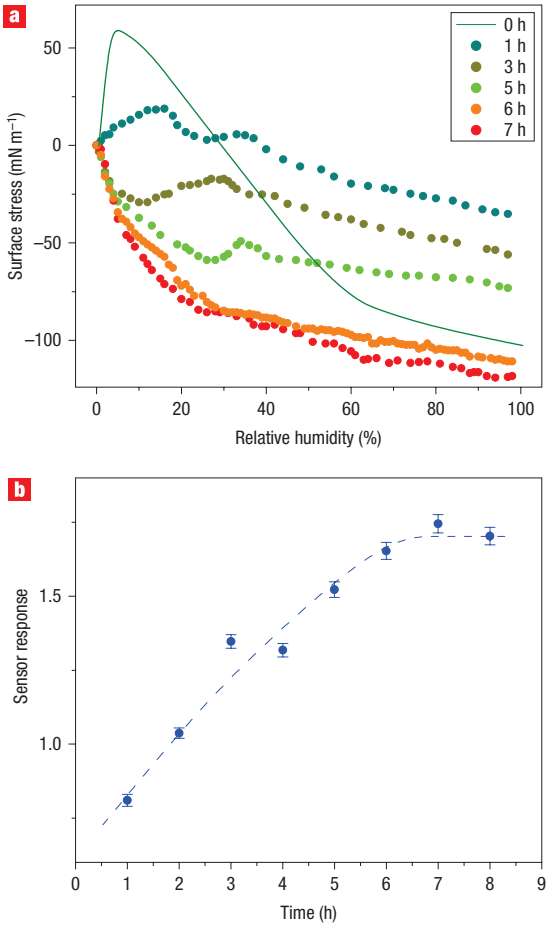

Figure 4 Hydration-induced surface stress as a function of hybridization time. a, Surface stress versus relative humidity for a ssDNA-sensitized cantilever exposed to a solution of 1 pM complementary ssDNA, as a function of the hybridization time. The experiment was performed by hybridizing, rinsing and drying the cantilever at different times. The response saturates for periods longer than 6 h. **b**, Sensor response (calculated as defined in the Methods) versus hybridization time.

was achieved after 6 h, and the response is similar to the equilibrium response for 1 μM of complementary DNA. This indicates that the density of hybridized probes is similar in both cases. For shorter incubation times, the most significant changes are produced at low humidity. For higher humidity (>40%) the surface stress variation is very similar for all curves. The initial surface stress change gradually evolves from positive values (tensile stress) to negative values (compressive stress). The surface stress response to the adsorption of the first water molecules can then be understood in terms of two competing interactions: the attractive forces driven by the hydrogen bonding (tensile stress) and the steric hindrance interactions (compressive stress). The dominant interaction is controlled by the size of the intermolecular channels and their blockade by the hybridized DNA molecules.

The hybridization curves before achieving equilibrium exhibit tensile peaks at relative humidities of 30–40% (Fig. 4a). These features are in fact beyond our current understanding. However, it is interesting to note a number of processes that can contribute to variations of the surface stress. First, it is well known that under limited hydration the structure of nucleic acids is different from their conformation under physiological conditions[22]. The most studied transition is between the B- and A-forms of the double-stranded DNA that occurs at limited hydration, although other transitions can also occur. The B-helix is narrower and more extended than its A counterpart and hence, in our system, the A → B transition as relative humidity increases should produce a decrease of the repulsive intermolecular interactions between neighbouring molecules. Another factor that adds complexity to the observed phenomenon is the slow hybridization kinetics in densely packed DNA monolayers[28].

© 2008 Nature Publishing Group

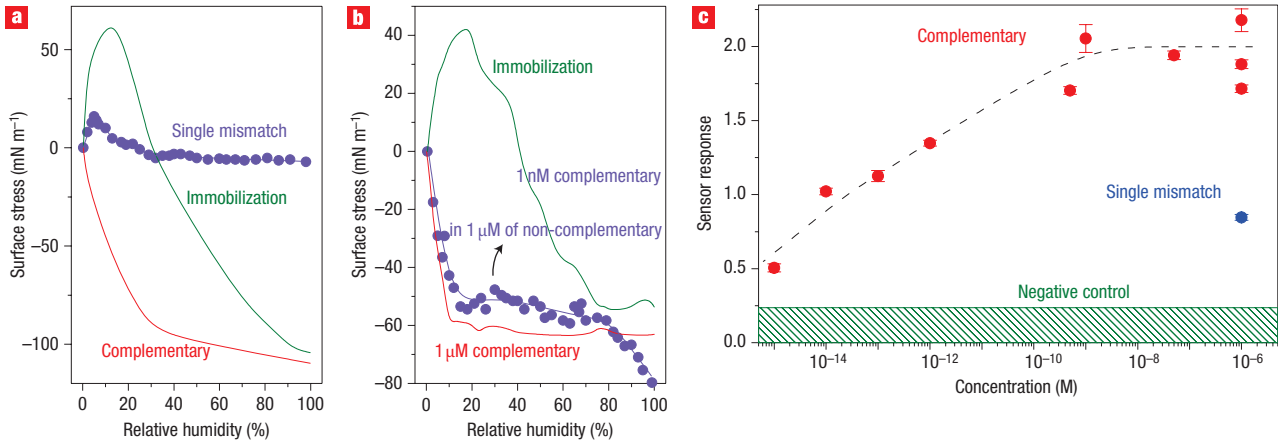

Figure 5 Specificity and sensitivity of the hydration-based DNA nanomechanosensor. a, Effect of a nucleotide mutation in the ssDNA target on the hydration-induced surface stress (violet symbols and line). The mismatched sequence promotes a single T/T central mismatch upon hybridization. The curve for the non-hybridized ssDNA-sensitized cantilever (green line), and that of the hybridization with the fully complementary sequence (red line) are also shown for comparison. The target concentration was 1 μM and the hybridization time 3 h. **b**, Surface stress upon hydration of a ssDNA-sensitized cantilever exposed to 1 nM of complementary target in the presence of 1 μM non-complementary DNA (violet symbols and line). The curve for the non-hybridized ssDNA-sensitized cantilever (green line) and that of the hybridization with 1 μM of the fully complementary sequence (red line) are shown. The hybridization time was 3 h. **c**, Plot of the sensor response (as defined in the Methods) as a function of the concentration of the complementary target ssDNA (red symbols). The sensor response given by hybridization with non-complementary ssDNA (negative control) is also plotted and used to indicate the floor lever of sensitivity (green dashed area). The sensor response for the mismatched sequence at 1 μM (derived from **a**) is also shown (blue symbol).

In these films, steric crowding leads to only ~10% of the immobilized probes being formed as a duplex with the complementary sequence[12,29]. In addition, the formation of the nucleation sites between the probe and the target before the zipping reaction is significantly hindered, and it can last several hours. Before achieving equilibrium, complementary ssDNA can be in two conformations: either completely zipped or joined to the ssDNA probe film by a few nucleations points. The non-zipped complementary DNA can disrupt the structure of the monolayer, partially blocking the nanochannels to the intercalation of water molecules.

Despite the complexity of the detected phenomena, there is an intimate connection between the hydration-induced stress of the DNA SAM and the biomolecular interactions within. This suggests an application as a novel label-free nucleic acid biosensor with high sensitivity. The most remarkable difference induced by the hybridization emerges at low relative humidity during hydration, where the positive peak belonging to the ssDNA progressively vanishes with the degree of hybridization. We have therefore calculated the area enclosed between the surface stress curves of the ssDNA film before and after hybridization from relative humidities of 0 to 20% (see inset of Fig. 2a). The upper relative humidity limit of 20% has been chosen as an optimal value for unambiguous detection of the hybridization process. It includes stage I for the ssDNA sensitized cantilevers, and stage I* after subsequent hybridization. The calculated area is normalized by dividing by the area enclosed by the surface stress curve before hybridization (see Methods). This parameter is referred to as the sensor response, hereafter. In Fig. 4b we plot sensor response as a function of hybridization time for a concentration of 1 pM of complementary DNA.

The specificity of the biosensor was evaluated by exposing ssDNA-sensitized cantilevers to two kinds of samples: (1) 1 μM of ssDNA target with a single central mutation that originates a T/T mismatch (see Methods), and (2) a mixture of 1 nM of complementary ssDNA and 1,000-fold excess of non-matching ssDNA. Figure 5a shows surface stress versus relative humidity for a cantilever exposed to the target with the single mismatch for 3 h. The surface stress variation for relative humidities of <20% lies between that of the ssDNA monolayer and that of the hybridization with the complementary target. An initial tensile stress reminiscent of stage I is still observed. As all the hybridization experiments were performed at 24 °C, significant variations are not expected in the hybridization yield of the fully complementary and single-mismatched sequence (the discriminatory temperature for this target is ~43 °C). This indicates that the initial hydration-induced stress is sensitive to the difference in the duplex conformation as a consequence of the presence of a single mismatch. A tentative explanation for this is that the initial tensile stress could arise from the stabilization of the mismatched bases in the duplex by hydrogen bonding with water molecules. This feature of the technique is relevant for genotyping applications. Contrary to DNA microarrays and other current biosensors, the differential behaviour of the mismatched target does not rely on its tendency to de-hybridize at an optimized, fine-tuned working temperature (usually in the range 40–60 °C), but on its hydration-dependent response at room temperature.

Figure 5b shows surface stress versus relative humidity when a cantilever is exposed to 1 nM of complementary DNA in a background of 1 μM non-complementary DNA. The hybridization curve is very similar to that obtained in a parallel experiment in which a sensitized cantilever was exposed to a pure solution with 1 μM of complementary sequence and completely different to that obtained by exposing the sensitized cantilever to a pure solution with 1 μM of non-complementary DNA. Therefore, this demonstrates that the technique has enough specificity for the discrimination of targets in complex mixtures, and, in particular, for the detection of minority genomes constituting only 0.1% of the total amount of genomes in the sample. This capability can be applied for the detection and follow-up of minority genomes in RNA virus populations that can influence the evolution of the

© 2008 Nature Publishing Group

infected patient, as recently documented for human immunodeficiency virus in clinical samples.

Sensitivity was studied by measuring sensor response as a function of the concentration of the complementary target for a hybridization time of 3 h (Fig. 5c). We include the data for the mismatched sequence with a single T/T central mismatch (Fig. 5a) and that obtained for a non-complementary DNA (negative control, see Supplementary Information). The sensor response is approximately constant for target concentrations higher than 0.5 nM. The signal decreases as the target concentration decreases up to the analysed value of 1 fM, which still remains about twice as high as the sensor response measured for the negative control. A key to obtain this extraordinary sensitivity is the high grafting density of the ssDNA monolayer, which leaves sub-nanometre intermolecular channels between. There is strong evidence that adsorption in nanoscale voids gives rise to stresses that may exceed the surface stress of smooth surfaces by several orders of magnitude[6]. The hybridization process therefore has an important impact on hydration-induced surface stress as it strongly modifies the capability of the molecular channels to store water molecules[27].

CONCLUSIONS

The unprecedented sensitivity observed here by measuring the nanomechanical response of nucleic acids films upon hydration has not previously been achieved by any biosensor able to detect unlabelled target samples. Earlier nanomechanical biosensors based on surface stress have detected nucleic acids with high sensitivity in buffer solution, providing real-time information about the hybridization kinetics[12,13]. In those reports, a clear cantilever bending emerges after a few minutes of interaction between the complementary sequences and the ssDNA probes on the cantilever. The hydration-based nanomechanical method proposed here does not provide real-time information and requires between 1 and 3 h incubation of the ssDNA- or ssPNA-sensitized cantilevers with the nucleic acid sample. However, the hybridization provides an enormous quantitative and qualitative change in the hydration-induced tension of the nucleic acid film. In fact, the use of reference cantilevers is not necessary to detect hybridization, a practice that is essential for measurements in buffer in order to remove non-specific signals from fluctuations in temperature and electrolyte concentration[15].

We demonstrate sensitivity in the fM range, which is an enhancement of three orders of magnitude with respect to previous nanomechanical methods using similar sizes of cantilever[13]. More importantly, there is potential for major improvements in sensitivity and throughput by measuring in parallel using hundreds of cantilevers with superior mechanical properties. In addition, the ultimate goal of a biosensor, the detection of a single molecule, is brought closer by miniaturization of the microscale cantilever to the nanoscale[9,11]. These results, together with previous developments in nanomechanical sensors, bring us closer to the use of this technology for genotyping and functional genomic research. The realization of these applications would allow the early diagnosis of diseases without the time-costly steps of amplification and labelling of the sample.

METHODS

PREPARATION OF ssDNA SAMPLES

ssDNA thiol-modified probes (with the 5′ modification HS-$(CH_2)_6$) and label-free ssDNA targets were obtained from Microsynth. DNA oligomers were HPLC purified and desiccated. Before use, the samples were resuspended in PBS buffer (137 mM NaCl, 2.7 mM KCl, 8 mM Na_2HPO_4, 2 mM KH_2PO_4; pH = 7.5) and divided in aliquots of the desired volume and concentration without further modifications. All solutions were prepared using Milli-Q water (18 MΩ cm^{-1}) and stored at −20 °C. The oligonucleotide sequences used were thiol-modified 16-mer probe 5′-HS-CTACCTTTTTTTCTG-3′, the fully complementary target (5′-CAGAAAAAAAAGGTAG-3′), the target T with a single mutation in its central region, which induces a T/T mismatch in the duplex (5′-CAGAAAA**T**AAAGGTAG-3′) and a non complementary target used as negative control (5′-AGCTTCCGTACTCGAT-3′).

DNA IMMOBILIZATION AND HYBRIDIZATION

Uncoated monocrystalline silicon microcantilever arrays were purchased from Mikromasch. The microcantilevers were 400 μm long, 100 μm wide and 0.6 μm thick. They showed a resonance frequency of 5.3 ± 0.1 kHz and a spring constant (calculated by Sader's method[30]) of 0.029 ± 0.001 N m^{-1}. The cantilevers were coated by e-beam evaporation with a 20-nm gold layer on top of a 2-nm adhesion layer of chromium at a deposition rate of 0.02 nm s^{-1}. Freshly coated microcantilevers were incubated with 1 μM of the ssDNA probe diluted in PBS at 24 °C for 24–48 h in order to immobilize a densely packed DNA layer to provide the hydration-induced surface stress curve shown in Fig. 1. Afterwards, the cantilevers were vigorously rinsed in PBS buffer and Milli-Q water to discard unspecific interactions. The duration of each washing stage was ∼20 min, and they were performed at the working temperature (24 °C). The cantilevers were then dried under a stream of dry nitrogen gas. The hybridization of the sensitized cantilever with the target ssDNA was performed in PBS at 24 °C, at the desired target concentration and hybridization time. Afterwards, the cantilevers were rinsed and dried following the same protocol used for the sensitized cantilevers. To study the nanomechanical cantilever response as a function of the hybridization time (as in Fig. 4), the same cantilever was exposed to the DNA target several times, followed by the steps of rinsing and drying described above.

PNA IMMOBILIZATION

An HPLC-purified ssPNA oligomer was used as the immobilization probe, with sequence (written from the amino to the carboxyl termini) cys-O-O-AATCCCCGCAT (Applied Biosystems). Each O spacer unit was a molecule of 8-amino-3,6-dioxaoctanoic acid, used to separate the hybridization portion of the molecule from its 5′ terminus. The overall length of the spacer formed by two consecutive O linkers was 3.0 nm. The terminal cysteine provides a thiol group that allows interaction with gold, following a method previously described[26]. The ssPNA solutions were prepared in Milli-Q water (18 MΩ cm^{-1}), where, contrary to the natural nucleic acids, PNA remains active and functional. Immobilization of ssPNA on the cantilevers was performed with a concentration of 1 μM at 24 °C for 24 h, by placing the chips in an Eppendorf tube containing a 10 μl drop of the ssPNA solution. After immobilization, the chips were vigorously rinsed in water and finally dried in nitrogen gas for 30 min. For hybridization experiments, the ssPNA-sensitized cantilever was exposed to the complementary ssDNA target (5′-ATGCGGGGATT-3′).

MEASUREMENT OF THE SURFACE STRESS

The nanomechanical response of the cantilevers was measured by using a home-built apparatus equipped with an environmental chamber (∼400 cm^3) and an optical readout technique that calculates the displacement of the cantilever at 30–50 positions along the cantilever longitudinal axis (see Supplementary Information). The temperature was controlled by means of a Peltier cell placed below the cantilever, with a temperature sensor close to it. The relative humidity in the chamber was controlled by adjusting the flow rates of dry nitrogen and wet nitrogen (nitrogen bubbling through a wash flask filled with water) by means of precision valves. The total flow rate was ∼500 ml min^{-1}. The relative humidity was changed at a rate of about 1% per minute. We did not find a significant change in the surface stress behaviour by varying this rate from 0.3 to 5% per minute. Before measuring the surface stress versus relative humidity, the cantilevers were equilibrated at a relative humidity of 0% in a flow of dry nitrogen for 1 h.

To calculate the surface stress, the cantilever profile was fitted to a second-order polynomial to deduce the curvature radius. The surface stress σ is related to the curvature radius R by Stoney's equation[7],

$$\sigma = \frac{E}{6(1-\upsilon)}\frac{T^2}{R} \qquad (1)$$

where E = 169 GPa is Young's modulus and υ = 0.27 is the Poisson coefficient of the silicon in the <110> direction. The cantilever thickness T was calculated

© 2008 Nature Publishing Group

from the measured value of the resonant frequency. The cantilever displacement was obtained by calibrating the position-sensitive detector response (On-Trak Photonics) to preset changes of angle between the cantilever and the detector (see Supplementary Information).

SENSOR RESPONSE QUANTIFICATION

The amount of hybridized probes was quantified by calculating the area enclosed between the immobilization and hybridization curves at relative humidities between 0 and 20% (see inset in Fig. 2a). This quantity was normalized by dividing by the area enclosed by the immobilization curve to minimize deviations due to variations in the mechanical properties of the cantilevers, gold coating and features of the ssDNA monolayer. The area enclosed by the curves was calculated by numerical integration of the experimental data. The processing of the data is described by the following equation:

$$\mathrm{SR} = \frac{\int_0^{20} \mathrm{d}x \left[\sigma_{\mathrm{immob}}(x) - \sigma_{\mathrm{hyb}}(x)\right]}{\int_0^{20} \mathrm{d}x \sigma_{\mathrm{immob}}(x)} \qquad (2)$$

where SR is the (adimensional) sensor response, σ is the surface stress variation with relative humidity, x is the relative humidity, and the subscripts immob and hyb denote the ssDNA-sensitized cantilever and that cantilever after hybridization, respectively. The error bars in Figs. 4b and 5c are calculated from the effect of the measurement error (measured from the signal fluctuations at a single humidity) on the sensor response (equation (2)).

Received 28 February 2008; accepted 13 March 2008; published 20 April 2008.

References

1. Israelachvili, J. & Wennerstrom, H. Role of hydration and water structure in biological and colloidal interactions. *Nature* **379**, 219–225 (1996).
2. Petrovykh, D. Y., *et al*. Nucleobase orientation and ordering in films of single-stranded DNA on gold. *J. Am. Chem. Soc.* **128**, 2–3 (2006).
3. Petrovykh, D. Y., Kimura-Suda, H., Whitman, L. J. & Tarlov, M. J. Quantitative analysis and characterization of DNA immobilized on gold. *J. Am. Chem. Soc.* **125**, 5219–5226 (2003).
4. Shu, W. *et al*. DNA molecular motor driven micromechanical cantilever arrays. *J. Am. Chem. Soc.* **127**, 17054–17060 (2005).
5. Thundat, T., Wachter, E. A., Sharp, S. L. & Warmack, R. J. Detection of mercury vapor using resonating microcantilevers. *Appl. Phys. Lett.* **66**, 1695–1697 (1995).
6. Lavrik, N. V., Sepaniak, M. J. & Datskos, P. G. Cantilever transducers as a platform for chemical and biological sensors. *Rev. Sci. Instrum.* **75**, 2229–2253 (2004).
7. Raiteri, R., Grattarola, M., Butt, H.-J. & Skládal, P. Micromechanical cantilever-based biosensors. *Sens. Actuators B* **79**, 115–126 (2001).
8. Burg, T. P. *et al*. Weighing of biomolecules, single cells and single nanoparticles in fluid. *Nature* **446**, 1066–1069 (2007).
9. Li, M., Tang, H. X. & Roukes, M. L. Ultra-sensitive NEMS-based cantilevers for sensing, scanned probe and very high-frequency applications. *Nature Nanotech.* **2**, 114–120 (2007).
10. Gupta, A., Akin, D. & Bashir, R. Single virus particle mass detection using microresonators with nanoscale thickness. *Appl. Phys. Lett.* **84**, 1976–1978 (2004).
11. Ilic, B. *et al*. Enumeration of DNA molecules bound to a nanomechanical oscillator. *Nano Lett.* **5**, 925–929 (2005).
12. McKendry, R. *et al*. Multiple label-free biodetection and quantitative DNA-binding assays on a nanomechanical cantilever array. *Proc. Natl Acad. Sci. USA* **99**, 9783–9788 (2002).
13. Zhang, J. *et al*. Rapid and label-free nanomechanical detection of biomarker transcripts in human RNA. *Nature Nanotech.* **1**, 214–220 (2006).
14. Wu, G. *et al*. Bioassay of prostate specific antigen (PSA) using microcantilevers. *Nature Biotechnol.* **19**, 856–860 (2001).
15. Calleja, M., Tamayo, J., Nordstrom, M. & Boisen, A. Low noise polymeric nanomechanical biosensors. *Appl. Phys. Lett.* **88**, 113901 (2006).
16. Bumbu, G. G., Wolkenhauer, M., Kircher, G., Gutmann, J. S. & Berger, R. Micromechanical cantilever technique — a tool for investigating the swelling of polymer brushes. *Langmuir* **23**, 2203–2207 (2007).
17. Reddy, M. R. & Berkowitz, M. Hydration forces between parallel DNA double helices: Computer simulations. *Proc. Natl Acad. Sci. USA* **86**, 3165–3168 (1989).
18. Rau, D. C., Lee, B. & Parsegian, V. A. Measurement of the repulsive force between polyelectrolyte molecules in ionic solution: Hydration forces between parallel DNA double helices. *Proc. Natl Acad. Sci. USA* **81**, 2621–2625 (1984).
19. Hagan, M. F., Majumdar, A. & Chakraborty, A. K. Nanomechanical forces generated by surface grafted DNA. *J. Phys. Chem. B* **106**, 10163–10173 (2002).
20. Antoniou, A. *et al*. Average risks of breast and ovarian cancer associated with BRCA1 or BRCA2 mutations detected in case series unselected for family history: a combined analysis of 22 studies. *Am. J. Hum. Genet.* **72**, 1117–1130 (2003).
21. Mertens, J., Álvarez, M. & Tamayo, J. Real-time profile of microcantilevers for sensing applications. *Appl. Phys. Lett.* **87**, 234102 (2005).
22. Tao, N. J., Lindsay, S. M. & Rupprecht, A. Structure of the DNA hydration shells studied by Raman spectroscopy. *Biopolymers* **28**, 1019–1030 (1989).
23. Schneider, B. & Berman, H. M. Hydration of the DNA bases is local. *Biophys. J.* **69**, 2661–2669 (1995).
24. Bryan, W. P. Thermodynamics of water–biopolymer interactions: irreversible sorption by a single uniform sorbent phase. *Biopolymers* **25**, 1967–1979 (1986).
25. Casanova, F., Chiang, C. E., Li, C.-P. & Schuller, I. K. Direct observation of cooperative effects in capillary condensation: the hysteretic origin. *Appl. Phys. Lett.* **91**, 243103 (2007).
26. Briones, C. *et al*. Ordered self-assembled monolayers of peptide nucleic acids with DNA recognition capability. *Phys. Rev. Lett.* **93**, 208103 (2004).
27. Mateo-Martí, E., Briones, C., Pradier, C. M. & Martín-Gago, J. A. A DNA biosensor based on peptide nucleic acids on gold surfaces. *Biosens. Bioelectron.* **22**, 1926–1932 (2007).
28. Hagan, M. F. & Chakraborty, A. K. Hybridization dynamics of surface immobilized DNA. *J. Chem. Phys.* **120**, 4958–4968 (2004).
29. Peterson, A. W., Heaton, R. J. & Georgiadis, R. M. The effect of surface probe density on DNA hybridization. *Nucleic Acids Res.* **29**, 5163–5168 (2001).
30. Sader, J. E. Calibration of rectangular atomic force microscope cantilever. *Rev. Sci. Instrum.* **70**, 3967–3969 (1999).

Supplementary Information accompanies this paper on www.nature.com/naturenanotechnology.

Acknowledgements

D.R. acknowledges the fellowship funded by the Autonomous Community of Madrid (CAM). J.T., M.C., J.M. and D.R. acknowledge financial support from the Spanish Ministry of Science (MEC) under grant TEC2006-10316 and CAM under grant 200550M056. C.B. acknowledges funding provided by MEC under grant BIO2007-67523. Work at Centro de Astrobiología was supported by the European Union (EU), Instituto Nacional de Técnica Aeroespacial (INTA), MEC and CAM. All the authors acknowledge A. Cebollada, J.M. García-Martín, J. García, J.L. Costa-Kramer, M. Arroyo-Hernández and J.V. Anguita for their assistance in carrying out the gold deposition on the cantilevers.

Author contributions

J.T., J.M. and M.C. designed the hydration experiments. J.T., J.M., D.R. and M.C. developed the measurement instrument. C.B., J.A.M.-G. and C.R. designed the PNA experiments for ruling out the effect of electrostatic forces. J.M., M.C. and C.R. carried out the experiments. All authors analysed the data. J.T., M.C., C.B. and J.A.M.-G. wrote the manuscript and all authors proofread it.

Author information

Reprints and permission information is available online at http://npg.nature.com/reprintsandpermissions/. Correspondence and requests for materials should be addressed to J.T.

© 2008 Nature Publishing Group